FEBS Letters 585 (2011) 3020–3025

FEBS Letters
journal homepage: www.FEBSLetters.org

# Structural basis of coagulation factor V recognition for cleavage by RVV-V

Daisuke Nakayama [a,b], Youssef Ben Ammar [a], Toshiyuki Miyata [b], Soichi Takeda [a,*]

[a] Department of Cardiac Physiology, National Cerebral and Cardiovascular Center Research Institute, 5-7-1 Fujishiro-dai, Suita, Osaka 565-8565, Japan
[b] Department of Molecular Pathogenesis, National Cerebral and Cardiovascular Center Research Institute, 5-7-1 Fujishiro-dai, Suita, Osaka 565-8565, Japan

ARTICLE INFO

*Article history:*
Received 6 June 2011
Revised 1 August 2011
Accepted 11 August 2011
Available online 23 August 2011

Edited by Christian Griesinger

*Keywords:*
Blood coagulation
Snake venom
Serine proteinase
Substrate recognition
Induced fit

ABSTRACT

**Russell's viper venom factor V (FV) activator (RVV-V) is a thrombin-like proteinase that specifically cleaves the Arg1545–Ser1546 bond of FV. Here we present the crystal structure of RVV-V in complex with the FV14 peptide (residues 1533–1546 of human FV) determined at 1.8 Å resolution. The structure reveals multiple interactions between RVV-V and the seven residues, Ile1539 ($P_7$)–Arg1545 ($P_1$), of the cleaved substrate. Comparison with substrate-free structures reveals conformational changes of the RVV-V loops upon substrate binding, suggesting that the multiple interactions are mediated by an induced-fit mechanism. The results provide an explanation for the narrow specificity of RVV-V.**


## 1. Introduction

FV is one of the key components of the blood coagulation cascade [1,2]. Human FV is a single-chain glycoprotein of 2190 amino acid residues and consists of six domains, A1, A2, B, A3, C1, and C2 [3]. FV circulates in the blood as a precursor molecule and is converted into the active form, FVa, after consecutive cleavage of the three peptide bonds, Arg709–Ser710, Arg1018–Thr1019, and Arg1545–Ser1546, by thrombin or activated factor X (FXa) [3–8]. These cleavages remove the highly glycosylated B domain from FV, resulting in the exposure of the binding site for FXa [9,10]. FVa acts as an essential cofactor in thrombin generation: the rate of the prothrombin-to-thrombin conversion by FXa is enhanced by several orders of magnitude in the presence of FVa and $Ca^{2+}$ on phospholipid membranes [6,11].

Snake venoms are rich sources of serine proteinases (SVSP) that exclusively belong to the MEROPS peptidase family S1, subfamily S1A (chymotrypsin-A subfamily) [12]. SVSPs interfere mostly with the hemostatic system upon envenomation [13]. Despite significantly high sequence identity (50–70%), SVSPs display high specificity toward distinct macromolecular substrates. RVV-V is an FV-activating SVSP isolated from Russell's viper venom [14]. RVV-V, which consists of 236 amino acids [15], cleaves only the Arg1545–Ser1546 bond of FV and does not cleave the other two thrombin-susceptible bonds [16]. Therefore, cleavage of FV by RVV-V does not release its B domain. However, FV cleaved by RVV-V acquires the ability to bind to FXa and shows the same level of procoagulant activity as FV activated by thrombin [4,17]. While thrombin acts on numerous proteins associated with hemostasis other than FV, no protein substrate other than FV has been identified for RVV-V to date. Prolonged incubation of RVV-V with factor VIII, fibrinogen, prothrombin and FX showed no apparent effects on either the structures or activities of these proteins [14,18]. This limited specificity of RVV-V toward FV among the components of blood clotting has made it an extremely useful tool in the investigation of FV both in the laboratory and for diagnostic purposes [19,20].

The present study reports the structure of RVV-V in a complex with the FV peptide and delineates the subsites on RVV-V. This is the first report of the crystal structure of an SVSP in complex with a fragment of its macromolecular substrate.

## 2. Materials and methods

Protein preparation and crystallization of the substrate-free and D-Phe-Pro-Arg-chloromethylketone (PPACK)-bound RVV-V were performed as described previously [21]. The synthetic *N*-acetylated 14-amino acid peptide (FV-14), Ac-S-R-D-P-D-N-I-A-A-W-Y-L-R-S, was purchased from Sigma–Aldrich, Japan. A 20-fold molar excess amount of FV14 was added to the concentrated RVV-V solution. Crystals were obtained within several days at 277 K by the sitting drop vapor diffusion method with the reservoir solution containing 20% w/v PEG3350 and 0.2 M zinc acetate at pH 6.0. Crystals were

* Corresponding author. Fax: +81 6 6835 5416.
*E-mail address:* stakeda@ri.ncvc.go.jp (S. Takeda).

0014-5793/$36.00 © 2011 Federation of European Biochemical Societies. Published by Elsevier B.V. All rights reserved.
doi:10.1016/j.febslet.2011.08.022

**Table 1**
Data collection and refinement statistics.

| | Substrate-free closed-form | Substrate-free open-form | PPACK-bound form | RVV-V/FV14 complex |
|---|---|---|---|---|
| PDB ID | 3S9A | 3S9B | 3SBK | 3S9C |
| **Data collection** | | | | |
| Space group | $P6_522$ | $P6_522$ | $P6_522$ | $P6_1$ |
| Cell dimensions | | | | |
| *a*, *b*, *c* (Å) | 78.9, 78.9, 157.3 | 80.1, 80.1, 160.4 | 77.2, 77.2, 168.4 | 101.2, 101.2, 44.2 |
| $\alpha$, $\beta$, $\gamma$ (°) | 90, 90, 120 | 90, 90, 120 | 90, 90, 120 | 90, 90, 120 |
| Wavelength (Å) | 1.0 | 1.0 | 1.0 | 1.0 |
| Resolution (Å) | 50.0–1.9 (1.97–1.90) | 50.0–1.9 (1.97–1.90) | 50.0–2.55 (2.64–2.55) | 30.0–1.8 (1.86–1.80) |
| No. of unique reflections | 23 547 (2301) | 24 182 (2389) | 10 311 (993) | 24 029 (2213) |
| $R_{merge}$ | 0.063 (0.255) | 0.050 (0.282) | 0.065 (0.267) | 0.047 (0.296) |
| $I/\sigma(I)$ | 22.8 (8.6) | 22.0 (7.1) | 33.8 (15.8) | 46.3 (6.9) |
| Completeness (%) | 99.8 (100.0) | 97.6 (99.5) | 99.7 (100.0) | 99.0 (91.8) |
| Redundancy | 7.0 (7.1) | 7.2 (7.2) | 20.4 (21.4) | 10.9 (9.3) |
| No. of protein molecules in ASU | 1 | 1 | 1 | 1 |
| **Refinement** | | | | |
| Resolution (Å) | 30.0–1.9 (1.97–1.90) | 30.0–1.9 (1.97–1.90) | 30.0–2.55 (2.62–2.55) | 30.0–1.8 (1.86–1.80) |
| No. reflections | 23544 (2274) | 24166 (2356) | 10255 (722) | 23944 (2204) |
| $R_{work}$ | 0.219 (0.240) | 0.198 (0.227) | 0.248 (0.354) | 0.183 (0.260) |
| $R_{free}$ | 0.254 (0.263) | 0.219 (0.290) | 0.330 (0.470) | 0.219 (0.292) |
| No. atoms | | | | |
| Protein | 1817 | 1817 | 1817 | 1881 |
| Carbohydrate | 14 | 14 | 14 | 39 |
| Water | 170 | 180 | 17 | 196 |
| Acetate | – | – | – | 16 |
| Zinc ion | – | – | – | 3 |
| Inhibitor | – | – | 30 | – |
| *B*-factors | | | | |
| Protein | 29.0 | 32.7 | 52.8 | 31.5 |
| Carbohydrate | 70.0 | 59.5 | 78.8 | 74.7 |
| Water | 38.1 | 41.9 | 36.3 | 43.6 |
| Acetate | – | – | – | 36.8 |
| Zinc ion | – | – | – | 33.5 |
| Inhibitor | – | – | 48.2 | – |
| R.M.S. deviations | | | | |
| Bond lengths (Å) | 0.005 | 0.006 | 0.010 | 0.011 |
| Bond angles (°) | 1.31 | 1.40 | 1.88 | 1.57 |
| Ramachandran[a] | | | | |
| Favored (%) | 96.55 | 97.41 | 93.99 | 97.89 |
| Outlier (%) | 0 | 0.43 | 0 | 0 |
| MolProbity score[a] | 1.79 (83rd percentile) | 1.63 (91st percentile) | 2.19 (92nd percentile) | 1.57 (91st percentile) |
| Clash score[a] | 11.25 (71st percentile) | 9.87 (77th percentile) | 19.43 (77th percentile) | 10.52 (70th percentile) |

Single crystals were used for each data set. Values in parentheses are for the highest-resolution shell.
[a] The accuracy of the models was judged by the MolProbity server [35].

cryoprotected by the reservoir solution supplemented with 20% glucose and 1 mM FV14 and were flash frozen under a stream of nitrogen gas at 100 K.

The diffraction data sets were collected at the SPring-8 beamline BL41XU by using the Rayonix MX225HE CCD detector at 100 K. Images were reduced using HKL2000 [22]. Structures were solved by the molecular replacement method. The structure of ACC-C (PDB ID: 2AIQ), a snake venom protein C activator that shares 61% sequence identity with RVV-V, was used as a starting model for solving the closed-form structure. The refined closed-form structure was used as a starting model for solving other structures. Refinements were performed by using CNS [23] and REFMAC [24]. The statistics of the data collection and refinement are summarized in Table 1. Interactions between RVV-V and FV were analyzed by the CCP4 programs and PDBe PISA [25]. Figures were generated by PyMOL [26].

RVV-V preparations have been shown to be a mixture of three isoforms [15]. Careful observations of the simulated-annealing omit electron-density maps around the six residues that differentiate the isoforms led to the conclusion that the major component in the crystal resolved was RVV-V-$\gamma$. By similar assessments, Glu148 and Asp149 were excluded from the reported RVV-V-$\gamma$ sequence [15] in our final models. The residue numbering in RVV-V is based on the topological equivalence to chymotrypsinogen.

## 3. Results and discussion

### 3.1. Overall structure

The overall structure of the RVV-V/FV14 complex is shown in Fig. 1A. RVV-V displays the typical fold of the chymotrypsin-A subfamily of serine endopeptidases. The catalytic triad is formed by the residues His57, Asp102 and Ser195 that are located at the interface of two six-stranded β-barrels.

The electron densities associated with FV14 are clearly observed for the seven residues from Ile1539 ($P_7$) to Arg1545 ($P_1$) (Fig. 1B), whereas the first 6 residues (Ser1533–Asn1538) are disordered in the crystal. The terminal carboxyl group is well defined and no connections were revealed in the electron density map. The terminal oxygens are adequately separated from the catalytic oxygen of Ser195 (3.0 and 3.1 Å) and form hydrogen bonds to the amide nitrogens of Gly193 and Ser195 and to the N$\varepsilon_2$ atom of

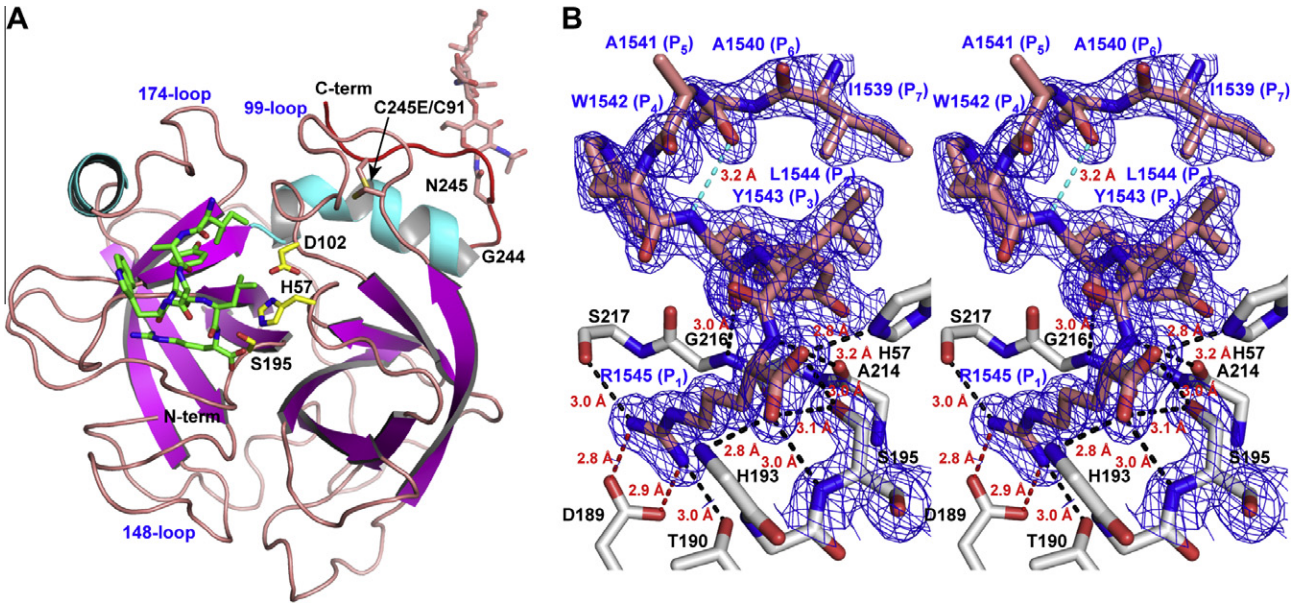


**Fig. 1.** Structure of the RVV-V/FV14 complex. (A) Ribbon representation of the RVV-V/FV14 complex. The FV residues Ile1539–Arg1545 and the side-chains of the active site residues in RVV-V are shown in green and yellow, respectively. RVV-V has a unique C-terminal nine residue extension (residues 244, 245, and 245A–245G shown in red) that contains an extra disulfide bond (Cys91–Cys245E) and an *N*-glycosylation site linked to Asn245, which is not found in thrombin or other mammalian serine proteinases. (B) Close-up view of the FV residues layered on the electron density map (simulated-annealing omit 2*Fo-Fc* map countered at 1.0$\sigma$) around the FV segment and Ser195 in RVV-V in stereo. The salt bridge and the hydrogen bonds between the atoms of FV14 (labeled in blue ink) and RVV-V (labeled in black ink) and the hydrogen bond within the FV14 are shown as dotted lines in red, black and cyan, respectively, with the atom–atom distances in red ink.

His57 (Fig. 1B). These observations confirm that RVV-V cleaves FV14 at the Arg1545–Ser1546 bond and suggest that the present structure represents an enzyme/product complex.

### 3.2. RVV-V subsites

The FV14 segment is bound to the $S_7$–$S_1$ subsites of RVV-V with a contact area of 687 Å$^2$ that accounts for 63.1% of its total solvent-accessible area of 1089 Å$^2$. This value is comparable with the reported 892 Å$^2$ between thrombin and the 10 residues of the fibrinopeptide [27] or the 602 Å$^2$ between granzyme M and its 6-residue catalytic product [28].

The side chain of Arg1545 ($P_1$) is bound in the deep $S_1$ pocket (Fig. 2A) via a salt bridge to the carboxyl group of Asp189 and also forms hydrogen bonds with the carbonyl oxygen of Ser217 and with the side-chain oxygen of Thr190 (Fig. 1B). Aside from the carboxyl oxygen described above, the amide nitrogen of Arg1545 forms a hydrogen bond with the carbonyl oxygen of Ala214. The Arg1545 residue is involved in 134 contacts that represent 41% of the total contacts formed between RVV-V and FV14 (Fig. 2B), suggesting that the $S_1$ specificity pocket functions as the primary subsite for FV recognition.

The side-chain of Leu1544 ($P_2$) makes contacts with the side-chain atoms of His57, Leu99 and Asp102 of RVV-V (Fig. 2C and D) that form the $S_2$ subsite, which is a part of the large cavity connecting the $S_3$ and $S_7$ subsites (Fig. 2A).

The side-chain of Tyr1543 ($P_3$) protrudes into the tunnel (Fig. 2A), the entrance of which is formed by the hydrophobic side-chains of Tyr172, Trp173, Val174, Ala214 and Val227 and the main-chain atoms of the residues Ala214-Gly216 of RVV-V (Fig. 2C and D). Of note, the indole ring of Trp173 is placed nearly perpendicular to the flat face of the phenyl ring of Tyr1543, forming contacts in a T-stacking configuration. The phenyl ring of Tyr1543 is sandwiched between the Nε atom of Trp173 and the Cα atom of Gly215, which are located 3.4 and 3.6 Å, respectively, from the Tyr1543 ring (Fig. 2C). In addition, the edge of the phenyl ring of Tyr1543 forms contacts with the flat face of the phenyl ring of Tyr172. The carbonyl oxygen of Tyr1543 forms a hydrogen bond with the amide nitrogen of Gly216 (Fig. 1B), which is the only hydrogen bond formed other than in the $P_1$–$S_1$ site. The hydroxyl group of Tyr1543 does not interact directly with the RVV-V atoms but it participates in the water-mediated hydrogen bond network formed inside the tunnel.

The flat face of the indole ring of Trp1542 ($P_4$) interacts with the edge of the indole ring of Trp173 in a T-stacking configuration on one hand, and its edge makes contact with the edge of the Tyr172 ring in RVV-V on the other (Fig. 2C). In addition to those aromatic interactions, the side-chain of Glu218 and the main-chain atoms of Leu171, Gly216 and Ser217 form multiple contacts with Trp1542 (Fig. 2C and D).

Ala1541 ($P_5$) interacts only with solvent molecules (Fig. 2A and B); therefore, RVV-V does not have an $S_5$ subsite.

Ala1540 ($P_6$) makes 11 contacts with the side-chain atoms of Trp173 (Fig. 2B and D).

Ile1539 ($P_7$) interacts with the side-chains of Phe95A, Asn97, Leu99 and Trp173 in RVV-V (Fig. 2C and D).

In summary, the $P_1$–$S_1$ recognition involves multiple interactions, including a salt bridge, hydrogen bonds and van der Waals interactions, whereas van der Waals contacts predominate in the $P_2$–$S_2$ to $P_7$–$S_7$ interactions. The RVV-V residues that interact with FV14 are perfectly conserved in the sequence of another FV-activating enzyme, LVV-V, isolated from *Daboia lebetina* venom [29] (Fig. 2D), with the exception of three residues. By careful observation, we confirmed that these substitutions do not interfere with FV-binding.

### 3.3. Flexibility of the RVV-V loops

The substrate-free RVV-V structures were determined in two distinct crystal forms at 1.9 Å resolution and the PPACK-bound RVV-V structure at 2.6 Å resolution. These structures are essentially identical to that of RVV-V in the RVV-V/FV14 complex with

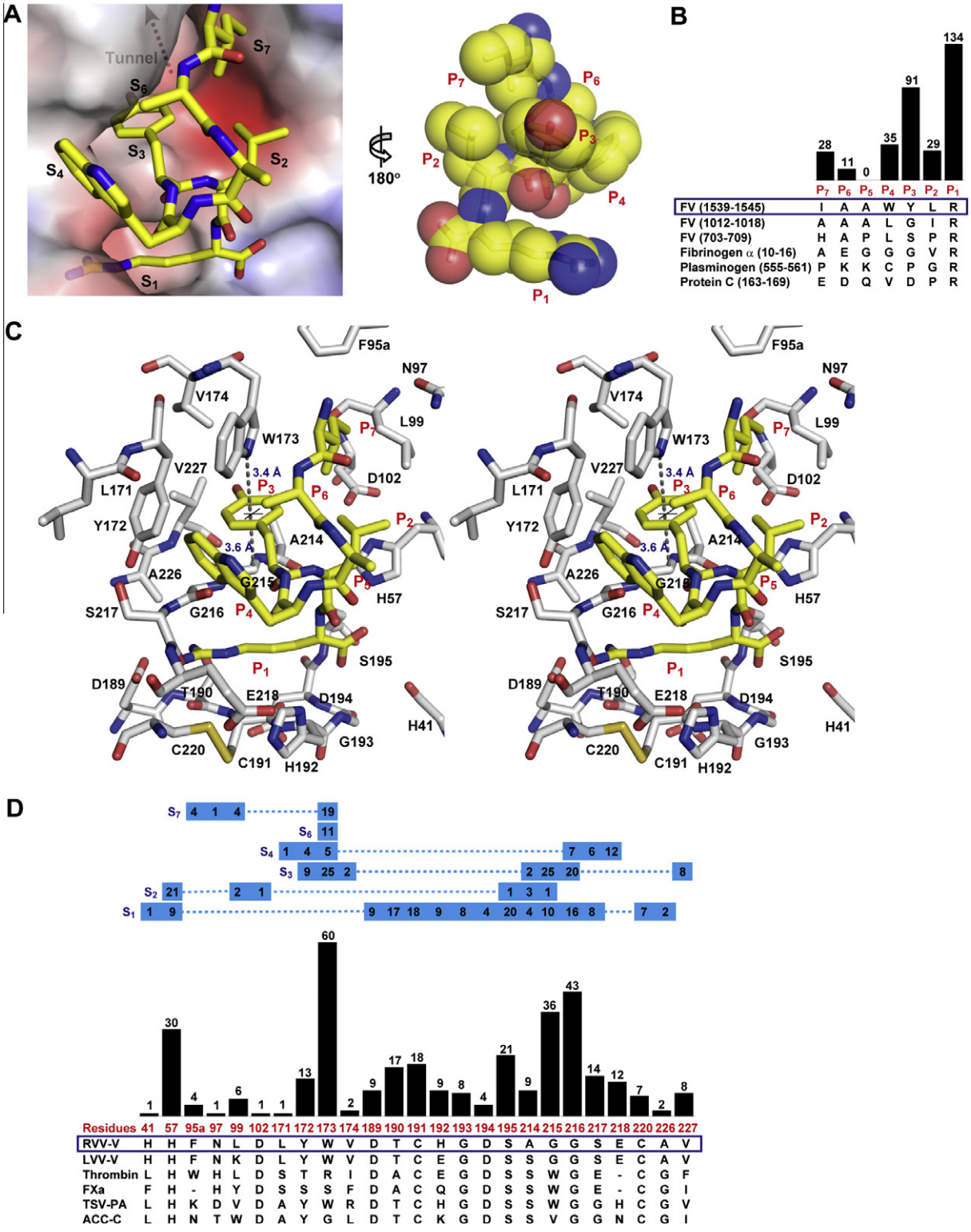


**Fig. 2.** Interactions between FV14 and RVV-V. (A) Subsites ($S_1$–$S_7$) are labeled on the molecular surface of RVV-V with the cognate FV residues shown in stick representation (left). Sphere representation with the van der Waal radius of each atom of the FV segment ($P_1$–$P_7$) viewed from the opposite side (right). (B) The number of contacts (pairs of atoms separated by less than 4.6 Å) between FV and RVV-V are plotted against the FV residues and the sequences of other thrombin-susceptible human proteins, as well as those of human plasminogen and protein-C, which are susceptible to TSV-PA and ACC-C, respectively. (C) Interactions between FV (shown in yellow and labeled in red ink) and RVV-V (shown in light gray and labeled in black ink) are shown in stereo. (D) The number of contacts between RVV-V and FV14 are plotted against the residues of RVV-V, LVV-V, human thrombin, FXa and SVSPs.

the exception of the loop configurations. The structure of the closed form of RVV-V shows significant differences in both the 99- and 174-loops in comparison to the structure of the FV14/RVV-V complex (Fig. 3A). As mentioned, Phe95a and Trp173 are directly involved in FV recognition by RVV-V and, of note, Trp173 provides the highest number of contacts among the RVV-V residues (Fig. 3D). In the absence of substrate-binding, these two aromatic rings are in proximity to each other and

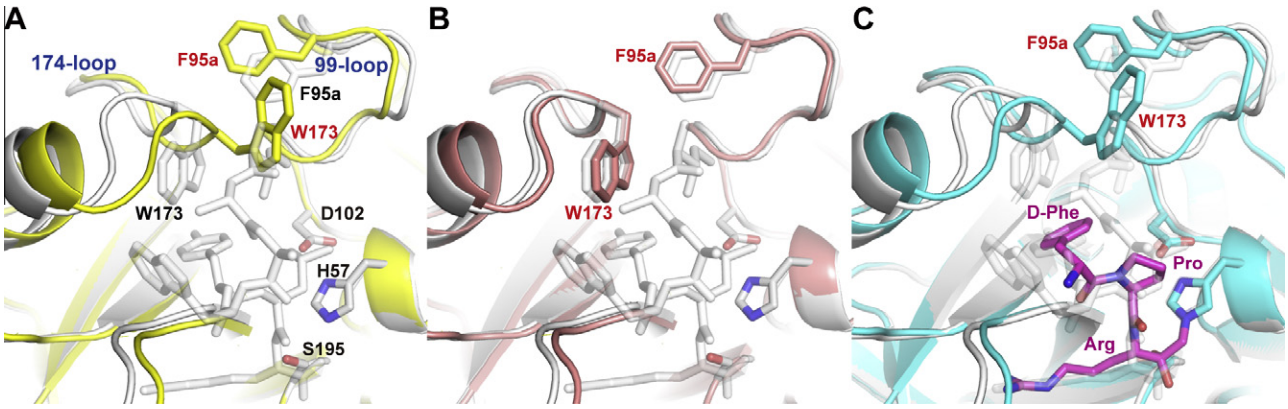


**Fig. 3.** Flexibility of the RVV-V loops. (A) Superimposition of the substrate-free closed-form (shown in yellow and labeled in red ink) and the RVV-V/FV14 complex structures (in light gray and labeled in black ink). (B) Superimposition of the open-form (shown in pink and labeled in red ink) and the RVV-V/FV14 complex structures. (C) Superimposition of the PPACK-bound form (shown in cyan and labeled in red ink) and the RVV-V/FV14 complex structures. PPACK is shown in magenta.

make a T-stacking contact, resulting in a closure of the $S_7$ subsite. On the other hand, RVV-V in the open-form adopts a similar structure to that of the RVV-V/FV14 complex (R.M.S.D. = 0.258) even in the absence of a bound substrate (Fig. 3B). The differences between these two substrate-free structures are solely caused by the crystal-packing effects, suggesting that the 99- and 174-loops are flexible in solution without substrate binding. In addition, in the PPACK-bound structure, the phenyl ring of the inhibitor interacts with the Cα atom of Gly215 with a similar geometry to that of Tyr1543 ($P_3$) in the RVV-V/FV14 complex but is not sandwiched by Trp173 because the 174-loop still represents a closed form-like structure (Fig. 3C). The binding of PPACK to RVV-V is similar to that of FV14 but is markedly different from the binding of thrombin [30].

### 3.4. Mechanism of FV recognition by RVV-V

In the RVV-V/FV14 complex, the main-chain of the FV segment adopts a partially extended conformation and has only one internal hydrogen bond that is formed between the carbonyl oxygen of Ala1540 and the amide nitrogen of Tyr1543 (Fig. 1B). However, the side-chain atoms of Leu1544, Tyr1543 and Ile1539 are tightly packed and collaboratively plug the large hydrophobic cavity formed by the continuous $S_2$, $S_3$ and $S_7$ subsites (Fig. 2A). The flexibility of the 174-loop and the fact that movement of Trp173 results in 28 additional contacts caused by the opening of the $S_7$ subsite (Fig. 2D) indicates that this plug is most likely formed by an induced-fit mechanism. Combination of the three hydrophobic residues at the $P_2$, $P_3$ and $P_7$ positions, which provides 148 contacts (45% of the total contacts between FV and RVV-V), is uniquely found in the Ile1539–Arg1545 segment of FV and not found in other thrombin-susceptible sequences (Fig. 2B). Therefore, the formation of this hydrophobic plug assembly could form part of the mechanism by which RVV-V specifically recognizes FV for cleavage at the Arg1545–Ser1546 bond.

Trp1542 ($P_4$) is also unique in the 1539–1545 segment of FV (Fig. 2B). As described, Trp1542 ($P_4$), together with Tyr1543 ($P_3$), forms multiple aromatic interactions with Tyr172 and Trp173 in RVV-V (Fig. 2C and D). This aromatic clustering may be an additional mechanism for FV recognition by RVV-V. Tyr172 and Trp173 are not conserved in thrombin and FXa but are found in TSV-PA, a plasminogen activating SVSP [31] (Fig. 2D). However, the TSV-PA-susceptible sequence is quite different from that of the 1539–1545 segment of FV (Fig. 2B), and the involvement of Tyr172 and Trp173 of TSV-PA in plasminogen recognition remains unclear.

Gly215 plays a critical role in FV recognition by RVV-V. The presence of non-Glycine residues at 215 severely hinders the binding of Tyr1543 ($P_3$) to the cognate subsite. Gly215 is uniquely found in RVV-V and LVV-V and is substituted by Trp in thrombin (Fig. 2D). The entrance of the $S_3$ tunnel identified in RVV-V is completely occupied by the Trp215 side-chain in thrombin [30]. Therefore, the above observations collectively suggest that the mechanism by which thrombin recognizes the Arg1545–Ser1546 bond of FV involves different interactions from those playing a role in RVV-V.

Trypsin-like proteinases and their zymogens undergo the rearrangement of the active site, which involves the transition from a disordered and flexible zymogen state to an ordered and rigid active enzyme state, following induced-fit substrate/inhibitor binding [32–34]. The present study clearly indicates that RVV-V undergoes substantial changes in the substrate-specificity pockets but only minimal changes both in catalytic triad and in the oxyanion hole upon substrate/inhibitor binding. The results suggest that a disorder-order transition of the catalytic site of RVV-V is mostly completed by the removal of an activation peptide during its maturation in the venom gland, however its activity and catalytic specificity are further regulated by induced-fit substrate binding.

## Acknowledgments

The authors thank M. Tomisako for her help in crystallization experiments. This work was supported in part by a Grant-in-Aid for Scientific Research from the Ministry of Education, Culture, Sports, Science and Technology and a Grant from the Naito Foundation.

## References

[1] Nicolaes, G.A. and Dahlback, B. (2002) Factor V and thrombotic disease: description of a janus-faced protein. Arterioscler. Thromb. Vasc. Biol. 22, 530–538.
[2] Mann, K.G. and Kalafatis, M. (2003) Factor V: a combination of Dr. Jekyll and Mr. Hyde. Blood 101, 20–30.
[3] Jenny, R.J., Pittman, D.D., Toole, J.J., Kriz, R.W., Aldape, R.A., Hewick, R.M., Kaufman, R.J. and Mann, K.G. (1987) Complete cDNA and derived amino acid sequence of human factor V. Proc. Natl. Acad. Sci. USA 84, 4846–4850.
[4] Suzuki, K., Dahlback, B. and Stenflo, J. (1982) Thrombin-catalyzed activation of human coagulation factor V. J. Biol. Chem. 257, 6556–6564.
[5] Esmon, C.T. (1979) The subunit structure of thrombin-activated factor V. Isolation of activated factor V, separation of subunits, and reconstitution of biological activity. J. Biol. Chem. 254, 964–973.
[6] Nesheim, M.E., Taswell, J.B. and Mann, K.G. (1979) The contribution of bovine factor V and factor Va to the activity of prothrombinase. J. Biol. Chem. 254, 10952–10962.
[7] Foster, W.B., Nesheim, M.E. and Mann, K.G. (1983) The factor Xa-catalyzed activation of factor V. J. Biol. Chem. 258, 13970–13977.

[8] Thorelli, E., Kaufman, R.J. and Dahlback, B. (1997) Cleavage requirements for activation of factor V by factor Xa. Eur. J. Biochem. 247, 12–20.
[9] Steen, M. and Dahlback, B. (2002) Thrombin-mediated proteolysis of factor V resulting in gradual B-domain release and exposure of the factor Xa-binding site. J. Biol. Chem. 277, 38424–38430.
[10] Toso, R. and Camire, R.M. (2004) Removal of B-domain sequences from factor V rather than specific proteolysis underlies the mechanism by which cofactor function is realized. J. Biol. Chem. 279, 21643–21650.
[11] Rosing, J., Tans, G., Govers-Riemslag, J.W., Zwaal, R.F. and Hemker, H.C. (1980) The role of phospholipids and factor Va in the prothrombinase complex. J. Biol. Chem. 255, 274–283.
[12] Rawlings, N.D., Barrett, A.J. and Bateman, A. (2010) MEROPS: the peptidase database. Nucleic Acids Res. 38, D227–D233.
[13] Serrano, S.M. and Maroun, R.C. (2005) Snake venom serine proteinases: sequence homology vs. substrate specificity, a paradox to be solved. Toxicon 45, 1115–1132.
[14] Schiffman, S., Theodor, I. and Rapaport, S.I. (1969) Separation from Russell's viper venom of one fraction reacting with factor X and another reacting with factor V. Biochemistry 8, 1397–1405.
[15] Tokunaga, F., Nagasawa, K., Tamura, S., Miyata, T., Iwanaga, S. and Kisiel, W. (1988) The factor V-activating enzyme (RVV-V) from Russell's viper venom. Identification of isoproteins RVV-V alpha, -V beta, and -V gamma and their complete amino acid sequences. J. Biol. Chem. 263, 17471–17481.
[16] Segers, K., Rosing, J. and Nicolaes, G.A. (2006) Structural models of the snake venom factor V activators from Daboia russelli and Daboia lebetina. Proteins 64, 968–984.
[17] Kane, W.H. and Majerus, P.W. (1981) Purification and characterization of human coagulation factor V. J. Biol. Chem. 256, 1002–1007.
[18] Esmon, C.T. and Jackson, C.M. (1973) The factor V activating enzyme of Russell's viper venom. Thromb. Res. 2, 509–524.
[19] Marsh, N. and Williams, V. (2005) Practical applications of snake venom toxins in haemostasis. Toxicon 45, 1171–1181.
[20] Perchuc, A.M. and Wilmer, M. (2010) Diagnostic use of snake venom components in the coagulation laboratory in: Toxins and Hemostasis: From Bench to bedside (Kini, R., Clemetson, K.J., Markland, F.S., McLane, M.A. and Morita, T., Eds.), pp. 747–766, Springer Science+Business Media.
[21] Nakayama, D., Ben Ammar, Y. and Takeda, S. (2009) Crystallization and preliminary X-ray crystallographic analysis of blood coagulation factor V-activating proteinase (RVV-V) from Russell's viper venom. Acta Crystallogr., Sect. F: Struct. Biol. Cryst. Commun. 65, 1306–1308.
[22] Otwinoski, Z. and Minor, W. (1997) Processing of X-ray diffraction data collected in oscillation mode.
[23] Brunger, A.T. et al. (1998) Crystallography and NMR system: A new software suite for macromolecular structure determination. Acta Crystallogr. D: Biol. Crystallogr. 54 (Pt 5), 905–921.
[24] Murshudov, G.N., Vagin, A.A. and Dodson, E.J. (1997) Refinement of macromolecular structures by the maximum-likelihood method. Acta Crystallogr. D: Biol. Crystallogr. 53, 240–255.
[25] Krissinel, E. and Henrick, K. (2007) Inference of macromolecular assemblies from crystalline state. J. Mol. Biol. 372, 774–797.
[26] DeLano, W.L. (2002) PyMOL Molecular Viewer. <http://www.pymol.org/>.
[27] Martin, P.D., Robertson, W., Turk, D., Huber, R., Bode, W. and Edwards, B.F. (1992) The structure of residues 7–16 of the A alpha-chain of human fibrinogen bound to bovine thrombin at 2.3-A resolution. J. Biol. Chem. 267, 7911–7920.
[28] Wu, L. et al. (2009) Structural basis for proteolytic specificity of the human apoptosis-inducing granzyme M. J. Immunol. 183, 421–429.
[29] Siigur, E., Aaspollu, A. and Siigur, J. (1999) Molecular cloning and sequence analysis of a cDNA for factor V activating enzyme. Biochem. Biophys. Res. Commun. 262, 328–332.
[30] Bode, W., Mayr, I., Baumann, U., Huber, R., Stone, S.R. and Hofsteenge, J. (1989) The refined 1.9 A crystal structure of human alpha-thrombin: interaction with D-Phe-Pro-Arg chloromethylketone and significance of the Tyr-Pro-Pro-Trp insertion segment. EMBO J. 8, 3467–3475.
[31] Zhang, Y., Wisner, A., Xiong, Y. and Bon, C. (1995) A novel plasminogen activator from snake venom. Purification, characterization, and molecular cloning. J. Biol. Chem. 270, 10246–10255.
[32] Bode, W. and Huber, R. (1976) Induction of the bovine trypsinogen–trypsin transition by peptides sequentially similar to the N-terminus of trypsin. FEBS Lett. 68, 231–236.
[33] Bode, W., Schwager, P. and Huber, R. (1978) The transition of bovine trypsinogen to a trypsin-like state upon strong ligand binding. The refined crystal structures of the bovine trypsinogen–pancreatic trypsin inhibitor complex and of its ternary complex with Ile-Val at 1.9 A resolution. J. Mol. Biol. 118, 99–112.
[34] Clausen, T., Kaiser, M., Huber, R. and Ehrmann, M. (2011) HTRA proteases: regulated proteolysis in protein quality control. Nat. Rev. Mol. Cell. Biol. 12, 152–162.
[35] Davis, I.W. et al. (2007) MolProbity: all-atom contacts and structure validation for proteins and nucleic acids. Nucleic Acids Res. 35, W375–W383.